



# Influence of the MWCNT surface functionalization on the thermoelectric properties of melt-mixed polycarbonate composites



Marco Liebscher<sup>a,b</sup>, Titus Gärtner<sup>a,b</sup>, Lazaros Tzounis<sup>a,b</sup>, Matej Mičušík<sup>c</sup>, Petra Pötschke<sup>a,\*</sup>, Manfred Stamm<sup>a,b</sup>, Gert Heinrich<sup>a,b</sup>, Brigitte Voit<sup>a,b</sup>

<sup>a</sup> Leibniz-Institut für Polymerforschung Dresden e.V., IPF, Hohe Str. 6, D-01069 Dresden, Germany

<sup>b</sup> Technische Universität Dresden, D-01062 Dresden, Germany

<sup>c</sup> Slovak Academy of Science (SAS), Polymer Institute, Dúbravská cesta 9, 845 41 Bratislava, Slovakia

## ARTICLE INFO

### Article history:

Received 30 April 2014

Received in revised form 2 July 2014

Accepted 6 July 2014

Available online 11 July 2014

### Keywords:

A. Carbon nanotubes

A. Nano composites

B. Electrical properties

B. Thermal properties

Thermoelectric properties

## ABSTRACT

The thermoelectric properties of conductive polymer composites consisting of a polycarbonate (PC) matrix loaded with different kinds of commercially available multi-walled carbon nanotubes (MWCNTs) have been examined. The PC/MWCNT composites were prepared by melt-mixing using a small-scale compounder. Unfunctionalized, as well as carboxyl (–COOH) and hydroxyl (–OH) modified MWCNTs were incorporated into the PC matrix at a constant amount of 2.5 wt.%, which is a concentration above the electrical percolation threshold. The amount of MWCNTs was kept low to understand the fundamental aspects of the physical properties and their correlation to the composite morphology. The results suggest that different functional groups on the surface of MWCNTs can have an impact on the thermoelectric values and the conductivity of the composites, measured at room temperature. The highest Seebeck coefficient ( $S$ ) was found for the composite containing carboxyl functionalized MWCNTs (11.3  $\mu\text{V/K}$ ). In specific, an increase of the Seebeck coefficient was found with an increased oxygen content of MWCNTs. It is believed that these thermoelectric figure of merit values are still too low for commercial applications; however, they can be enhanced by increasing the amount of conducting fillers and improvement of dispersion in the polymer matrix.

© 2014 Elsevier Ltd. All rights reserved.

## 1. Introduction

Nowadays, there is a huge concern regarding the finite supply of fossil fuels. Thermoelectric materials are one potentially alternative resource, specifically for thermal energy harvesting (such as waste heat), due to their ability to generate voltage upon exposure to temperature gradients relative to the environmental temperature. This so-called thermoelectric or Seebeck effect is described by the thermoelectric power (TEP), or thermopower, or Seebeck coefficient ( $S$ ), which is the direct solid state conversion of thermal energy to electricity [1]. The thermoelectric power is defined as:

$$S = \frac{\Delta V}{\Delta T} \quad (1)$$

where  $\Delta V$  is the electric potential difference (or the generated thermovoltage) created by a temperature gradient,  $\Delta T$ , to which the material is exposed. The Seebeck coefficient is used for the calculation of the power factor ( $PF$ ;  $PF = \sigma \times S^2$ ,  $\sigma$  is the electrical

conductivity), a well-known entity for comparing the efficiency of different thermoelectric materials. The dimensionless thermoelectric figure of merit ( $ZT$ ;  $ZT = \frac{\sigma S^2}{\kappa} T$ ,  $\kappa$  is the thermal conductivity and  $T$  the absolute temperature) is also used as a common measure to determine the materials' energy conversion efficiency [2,3]. The Seebeck coefficient is an intrinsic property of the materials related to their electronic properties and independent of their geometry [4]. Moreover, it is positive for p-type semi-conductors and negative for the n-type ones. Taking into account the previous equation of the thermoelectric figure of merit, it can be easily realized that for an efficient thermoelectric material, high electrical conductivity and high Seebeck coefficient, as well as low thermal conductivity are generally required. The low thermal conductivity is necessary so that the temperature gradient can be sustained within the material's structure and induces the generation of charge carriers. Traditional thermoelectric materials are made from low band gap semiconductors like  $\text{Bi}_2\text{Te}_3$ ,  $\text{PbTe}$ , etc. However, they are expensive to mass production, often toxic and consist of rare and expensive elements [3].

Recently, polymer based thermoelectrics have been reported and investigated both theoretically [5] as well as experimentally [6,7]. In addition, carbon nanotubes (CNTs) have shown promising

\* Corresponding author. Tel.: +49 (0)351 4658 395.

E-mail address: [poe@ipfdd.de](mailto:poe@ipfdd.de) (P. Pötschke).

thermoelectric behavior which has been found to be related to the level of doping [8,9] as well as the dopant nature [10–14]. Accordingly, several studies exist in which polymer/CNT composites have been utilized for the thermal energy harvesting [3,5,15–18]. Especially CNT-based polymer composites are of particular interest due to their low thermal conductivity, potentially high electrical conductivity, ease of production, relatively low cost, flexibility and high specific properties. The CNT networks in a polymer matrix have the ability to allow electron transport by tunneling, when junctions are separated by an insulating polymer film (even of some nm thick). At the same time, phonon scattering at the CNT–polymer–CNT interfaces will prevent their effective transmission through the composite resulting in low thermal conductivity values. Therefore, it can be concluded that polymer/CNT composites should fulfill well the demands for an efficient thermoelectric material taking into account the previous formula of the thermoelectric figure of merit. In almost all of the corresponding studies, polymer/CNT composites have been fabricated by means of solution mixing techniques which are known not to be easy in terms of up-scaling. Relatively high filler loadings ( $\gg 50$  wt.%) can be realized [18], which result in quite high electrical conductivities [19–23], while power factors being in the range of  $\sim 140 \mu\text{W/mK}^{-2}$  have been reported for single-walled carbon nanotubes (SWCNTs) in poly(3,4-ethylenedioxythiophene):poly(styrene sulfonate) (PEDOT:PSS) matrix [24]. However, such high filler loadings may result also in a significant increase of thermal conductivity [17,25,26]. One often reported approach for thermoelectric CNT-polymer composites is using electrically conductive matrix polymers, such as polyaniline (PANI) [21,23,24,27], polythiophene (PT), and PEDOT [19,24]. Their use can result in polymer composites with electrical conductivities up to  $4 \times 10^5 \text{ S/m}$  as reported by Moriarty et al. [24]. Doping of the SWCNTs by using e.g. polyethyleneimine (PEI) or hexafluoroacetone [28,29] resulted in Seebeck coefficients up to  $-50 \mu\text{V/K}$ . Furthermore, Seebeck coefficients between 10 and  $30 \mu\text{V/K}$  were reported for polythiophene/multi-walled carbon nanotube (MWCNT) and PANI/graphite composites [16,27].

Hewitt et al. showed Seebeck coefficients of MWCNT buckypapers between 11 and  $19 \mu\text{V/K}$ , and also discussed the dependence of the Seebeck coefficient on the MWCNT acid treatment procedure [30]. It was shown that acids with an oxygen content, such as sulfuric acid ( $\text{H}_2\text{SO}_4$ ) and nitric acid ( $\text{HNO}_3$ ), cause an increase of the Seebeck coefficient. For acids without oxygen, such as hydrochloric acid (HCl), no influence was shown. In addition, the duration of treatment, and the molarity of the acid exhibited a significant influence as well. Just recently, it has been reported that different dopants can change drastically the thermoelectric behavior of SWCNTs [14]. For composites of SWCNTs and PC prepared by solvent mixing, it was shown that by increasing the SWCNT content (up to 30% mass concentration), the electrical conductivity increases to approximately  $1000 \text{ S/m}$  [28]. Additionally, the Seebeck coefficient reached the value of  $60 \mu\text{V/K}$  and was found to be only slightly dependent on the SWCNT content. Furthermore, Seebeck coefficients up to  $10 \mu\text{V/K}$  were reported for expanded graphite and PC, which could be slightly improved up to  $12 \mu\text{V/K}$  by using additional polymers (PEDOT and PSS) [31]. In CNT based composites, polymers having electron rich functional groups, like PVA and PEI, have been found to act as n-doping to the incorporated SWCNTs, what resulted in coefficients up to  $-21.5 \mu\text{V/K}$  [29]. Studies using other preparation methods apart from solvent mixing are rare in literature. Antar et al. reported about melt-mixed composites of polylactide (PLA)/MWCNTs and expanded graphite [26]. In this study, high filling levels of up to 30 wt.% resulted in electrical conductivities of about  $4000 \text{ S/m}$ . However, a strongly increased thermal conductivity to  $5.5 \text{ W/m K}^{-1}$  was also reported. The Seebeck coefficient reached a maximum of  $17 \mu\text{V/K}$

for composites with expanded graphite and about  $9 \mu\text{V/K}$  for MWCNT composites. Beside this study, almost no work is reported about the thermoelectric behavior of polymer/CNT composites prepared by melt-mixing. In our previous work, it could be shown that for melt-mixed PC/MWCNT composites an increasing filler content results in an increase of the thermoelectric figure of merit due to high electrical conductivity and low remaining thermal conductivity [32].

In this study, a special focus is given on the influence of the functional groups of the MWCNTs on the thermoelectric properties of the resulting polycarbonate based polymer composites. The filler loading was kept at a low level to understand the relation between the physical properties and the morphology of the polymer composites. The electrical and thermal conductivity, as well as the Seebeck coefficient of the composites were determined and discussed in detail. Furthermore, the morphology of the composites was characterized and taken into account for the evaluation of the physical properties.

## 2. Experimental

### 2.1. Materials

The polycarbonate type Makrolon® PC 2205 (Bayer Material-Science, Leverkusen, Germany) with a density of  $1.2 \text{ kg/m}^3$  and a melt volume rate (MVR) of  $34 \text{ cm}^3/10 \text{ min}$  was used as the polymer matrix. Three different commercially available MWCNTs, namely Nanocyl™ NC3150, NC3151 and NC3153 were obtained from Nanocyl S. A. (Sambreville, Belgium). All MWCNT grades were produced via catalytic chemical vapor deposition processes (CCVD), and have purity higher than 95%. The NC3150 grade is reported as unfunctionalized MWCNTs (u-MWCNT), while the NC3151 and NC3153 were functionalized with carboxyl (MWCNT–COOH) and hydroxyl (MWCNT–OH) groups, respectively.

### 2.2. Sample preparation

For the compounding, a DSM Xplore 15 micro compounder (Geleen, Netherlands) with conical twin-screws was used. Prior to compounding, drying of both components was carried out at  $100^\circ\text{C}$  under vacuum overnight. The mixing process was performed at  $300^\circ\text{C}$  under a constant rotation speed of 150 rpm for a time period of 5 min. Preliminary thermogravimetric analysis (TGA) of MWCNTs, a known technique to characterize carbon nanotubes with respect to the different structural forms and the existence of reactive side-wall functional groups [33], has shown that the processing temperature slightly affected the MWCNT functional groups (data given in ESI). As reference, the unfunctionalized MWCNTs (u-MWCNTs) were used. In order to compare different functionalizations of MWCNTs, MWCNT–COOH and MWCNT–OH have been utilized. The amount of MWCNTs introduced in the PC matrix was kept constant at 2.5 wt.%. Hereafter, the PC composites containing u-MWCNTs, MWCNT–COOH and MWCNT–OH are denoted as PC/u-MWCNT, PC/MWCNT–COOH and PC/MWCNT–OH, respectively. To obtain samples for defined electrical conductivity measurements, the extruded strands were cut into short pieces and pressed under vacuum at  $300^\circ\text{C}$  into circular plates of 25 mm diameter and 0.8 mm thickness using a Weber press (PW 20, Paul Otto Weber; Remshalden, Germany). The compression molding temperature corresponded to the mixing temperature while the pressure was set for all samples at 17.5 kN. Subsequently, the temperature control was stopped, and the cooling process started. For the thermal conductivity measurements, different disk geometry was required. For this purpose, the compression molding device of the Weber press (PW 40, Paul Otto Weber; Remshalden, Germany) was used, while the pressure was

set to 50 kN for two minutes at the temperature of 300 °C. The subsequent cooling of the plates was carried out in a mini chiller. These plates had a diameter of 12.5 mm and a thickness of 2 mm.

### 2.3. Characterization

#### 2.3.1. XPS analysis of the MWCNTs

XPS signals for the different MWCNT types were recorded using a Thermo Scientific K-Alpha XPS system (Thermo Fisher Scientific, UK) equipped with a micro-focused, monochromatic Al K $\alpha$  X-ray source (1486.6 eV). An X-ray beam of 400  $\mu$ m size was used at 6 mA  $\times$  12 kV. The spectra were acquired in the constant analyzer energy mode with pass energy of 200 eV for the survey. Narrow regions were collected with pass energy of 50 eV. Charge compensation was achieved with the system flood gun that provides low energy electrons ( $\sim$ 0 eV) and low energy argon ions (20 eV) from a single source. The argon partial pressure was  $3 \times 10^{-7}$  mbar in the analysis chamber. The Thermo Scientific *Avantage* software, version 4.87 (Thermo Fisher Scientific), was used for digital acquisition and data processing. Spectral calibration was determined by using the automated calibration routine and the internal Au, Ag and Cu standards supplied with the K-Alpha system.

The surface compositions (in atomic %) were determined by considering the integrated peak areas of detected atoms and the respective sensitivity factors. The fractional concentration of a particular element A was computed using the following formula:

$$\%A = \frac{I_A/s_A}{\sum(I_n/s_n)} \times 100\% \quad (2)$$

where  $I_n$  and  $s_n$  are the integrated peak areas and the Scofield sensitivity factors corrected for the analyzer transmission, respectively.

#### 2.3.2. Morphological analysis of the composites

The morphological characterization was done on the extruded strands, perpendicular to the melt flow direction. The quantification of the MWCNT macro-dispersion in the polymer matrix was carried out by light optical microscopy (OM). Thin sections of  $\sim$ 5  $\mu$ m thickness were cut from the extruded strand at room temperature using a Leica RM2265 microtome (Leica Microsystems GmbH, Wetzlar, Germany). An Olympus BH2 microscope in transmission mode, combined with a DP71 video camera (Olympus Germany GmbH; Hamburg, Germany), was used for the section imaging. The state of dispersion was determined by analyzing the remaining, black appearing MWCNT agglomerates in the recorded image. These were quantified by calculating the agglomerate area ratio ( $A_A$ ) using the ImageJ 1.47n software. At least 10 individual recorded images at the same magnification were used for the calculations. To exclude impurities that were introduced during sample preparation or observation, particles with a circle equivalent diameter lower than 5  $\mu$ m were excluded from the calculation of the  $A_A$ .

Transmission electron microscopy (TEM) images were recorded in order to evaluate the MWCNT nano-dispersion. Ultrathin sections of the polymer composites with a thickness of  $\sim$ 70 nm were prepared by using an ultramicrotome (Leica UC7, Leica Microsystems GmbH, Wetzlar, Germany) at room temperature. The TEM images were acquired using the Libra200 (Carl Zeiss AG, Oberkochen, Germany) electron microscope operating at an acceleration voltage of 200 kV.

#### 2.3.3. Electrical and thermal conductivity measurements of the composites

Electrical resistivity measurements were performed on strips (18  $\times$  2 mm) mechanically punched from the compression molded plates with the dimensions of 25 mm diameter and 0.8 mm thickness (details for the plates preparation are given in Section 2.2). For

all the measurements, a Keithley 6517A electrometer (Keithley Instruments Inc., Cleveland, USA) applying 1 V was used combined with a 4-point measurement cell (external source electrodes spacing 16 mm and measuring electrodes spacing 10 mm). The presented conductivity values are derived from the corresponding reciprocal resistivity values. The thermal conductivity was measured using the Netzsch LFA 447 Nano Flash (Netzsch equipment manufacturing GmbH, Selb, Germany) on samples with a disk geometry having a diameter of 12.5 mm and a thickness of 2 mm (details for the plates preparation are given in Section 2.2). Both electrical as well as thermal conductivity measurements were carried out at room temperature.

#### 2.3.4. Thermoelectric power measurements

For the determination of the Seebeck coefficient, a self-made set-up developed at the Leibniz Institute of Polymer Research Dresden (IPF) was used. Composite strips of 2–3 mm width and 20–25 mm length (mechanically punched from the compression molded plates with the dimensions of 25 mm diameter and 0.8 mm thickness; details for the plates preparation are given in Section 2.2) were mounted on two metal blocks which allow the generation of a temperature gradient. For all measurements, one block was kept at room temperature ( $\sim$ 298 K), while the other one was heated up in a controlled way in 10 K steps up to 373 K. The distance between the two blocks was set to 15 mm. The generated electric potential difference, or thermovoltage ( $\Delta V$ ), was measured across the electrodes by a Keithley 6517A (Keithley Instruments Inc., Cleveland, USA) interfaced with a computer. The temperature of the two blocks was continuously measured with K-type thermocouples to determine the temperature gradient,  $\Delta T$ . The Seebeck coefficient was derived from the slope of  $\Delta V$  vs  $\Delta T$  curves by linear fitting, and the power factors have been calculated. Fig. 1a shows schematically the experimental set-up used for the thermoelectric power measurements, while Fig. 1b demonstrates the experimental apparatus.

## 3. Results and discussion

### 3.1. Chemical composition analysis of the commercial MWCNTs

The XPS results of unfunctionalized, carboxyl and hydroxyl functionalized MWCNTs are summarized in Table 1. It can be observed that different types of MWCNTs show different chemical compositions as reported also in other studies [34]. However, the unfunctionalized MWCNTs and MWCNTs with hydroxyl groups show very similar low amounts of oxygen and the C 1s and O 1s narrow regions were almost identical as well (see ESI). Only the MWCNT-COOH exhibit a relatively high amount of oxygen. More details related to the performed XPS analysis could be found in the ESI data. In a previous study, the XPS investigations for the same MWCNTs revealed quite similar results [35].

### 3.2. Microstructure investigations of the composites

Fig. 2 depicts the optical micrographs of the PC/MWCNT composites. It is clear that under constant mixing conditions the unfunctionalized MWCNTs (u-MWCNTs) show the best dispersion within the PC matrix, while the carboxyl modified ones (MWCNT-COOH) show the worse. The hydroxyl functionalized MWCNTs (MWCNT-OH) show also a very good dispersion in the PC matrix, and it is envisaged that the polymer melt can better infiltrate the MWCNT agglomerates compared to the carboxyl modified ones. This observation is also proven quantitatively with the determination of the  $A_A$ . The PC/u-MWCNT composite shows a relatively low  $A_A$  of 0.5% (Fig. 2, left side). For the composites containing



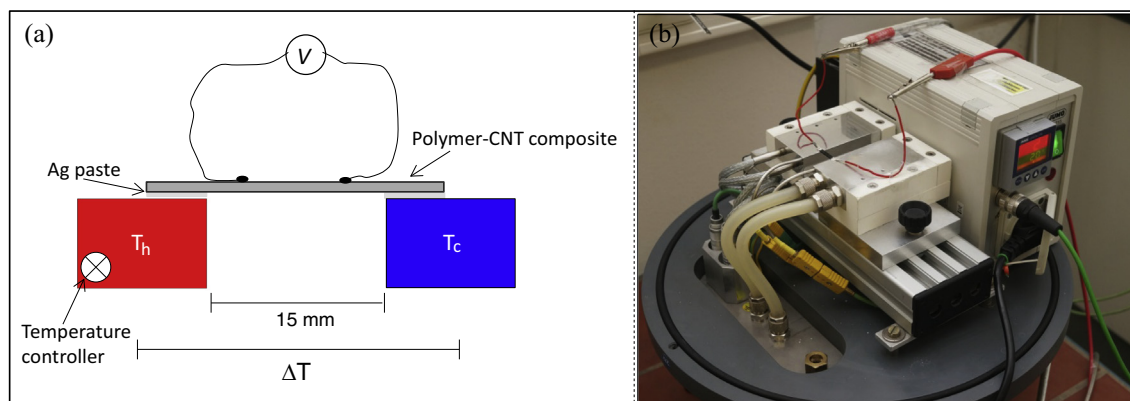


**Fig. 1.** (a) Schematic illustration of the experimental set-up used for the thermoelectric measurements and (b) a photo of the set-up.

**Table 1**

Chemical composition (in at.%) for the different MWCNTs as determined by XPS.

MWCNTs	Functional group	C 1s	O 1s
NC3150	Unfunctionalized	99.3	0.7
NC3151	–COOH	93.7	6.3
NC3153	–OH	99.3	0.7

MWCNTs with functional groups, the dispersion is generally worsened. In specific, the  $A_A$  of PC/MWCNT–COOH was calculated to be 7.4% (Fig. 2, middle), while for the PC/MWCNT–OH a value of 3.2% resulted (Fig. 2, right side). Similar results concerning the dispersion of the same functionalized MWCNTs have been reported recently for PVDF/MWCNT composites [36].

Fig. 3 depicts the TEM images of the different PC/MWCNT composites showing the MWCNT percolated network within the polymer matrix in more details. For all the samples, relatively well dispersed and homogeneously distributed MWCNTs can be observed. In specific, PC/u-MWCNT and PC/MWCNT–OH show similar states of dispersion, however slightly worse distribution was found for the carboxyl functionalized MWCNTs. The TEM micrographs seem to be in a good agreement with the observations of the optical microscopy analysis.

### 3.3. Electrical and thermal conductivity of the composites

The electrical conductivity of the prepared composites is presented in Fig. 4. All the composites were electrically conductive. The PC/u-MWCNT showed  $6.9 \pm 5$  S/m, while the PC/MWCNT–OH with slightly worse macro-dispersion reached a very similar conductivity of  $7.3 \pm 2.6$  S/m. The PC/MWCNT–COOH had the lowest conductivity of  $1.7 \pm 1.22 \times 10^{-2}$  S/m, attributed to the MWCNT

network characteristics observed previously by OM and TEM. Furthermore, possible defects introduced from the modification process to the MWCNT aromatic structure can destroy the  $sp^2$  hybridization of carbon having also a negative impact on the electronic properties of MWCNTs. The electrical conductivity values fully corroborate with the composite morphological characteristics observed by OM and TEM.

The thermal conductivity of the composites is shown in Table 2 indicating very low values in the range of  $0.3 \text{ W/m K}^{-1}$ . This low thermal conductivity is an important characteristic for the utilization of the MWCNT polymer composites as efficient thermoelectric materials. In our previous studies, it was already shown that even with 15 wt.% MWCNT loading the thermal conductivity remains below  $0.6 \text{ W/m K}^{-1}$  for melt-mixed PC composites [32]. These low values can be more precisely explained by phonon scattering occurring at the nanointerfaces preventing the effective transmission through the composite. Therefore, the temperature gradient is sustained within the material being the driving force of the temperature induced charge carriers.

### 3.4. Seebeck coefficient ( $S$ ), power factor ( $PF$ ) and thermoelectric figure of merit ( $ZT$ )

Fig. 5 demonstrates the Seebeck coefficients for the different samples. The Seebeck coefficient was found to be  $7.46 \pm 0.93 \mu\text{V/K}$  for the PC/u-MWCNT,  $11.34 \pm 1.24 \mu\text{V/K}$  for the PC/MWCNT–COOH, and  $8.44 \pm 0.22 \mu\text{V/K}$  for the PC/MWCNT–OH composite. It is easily observed that the PC/MWCNT–COOH exhibits the highest Seebeck coefficient which can be attributed to the high oxygen amount of the carboxylated MWCNTs acting as a p-dopant. It should be mentioned that the carboxyl groups facilitate the electron withdrawing from the MWCNT backbone, therefore, holes

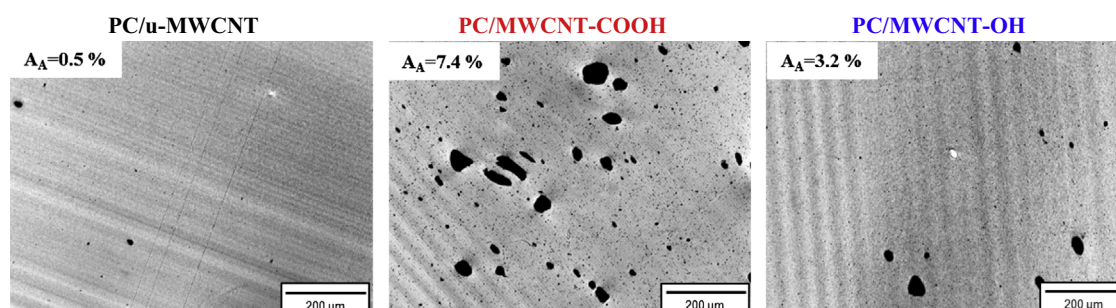


**Fig. 2.** Optical micrographs of the PC/MWCNT composites with 2.5 wt.% filler showing different states of MWCNT dispersion due to different functional groups of the MWCNTs.

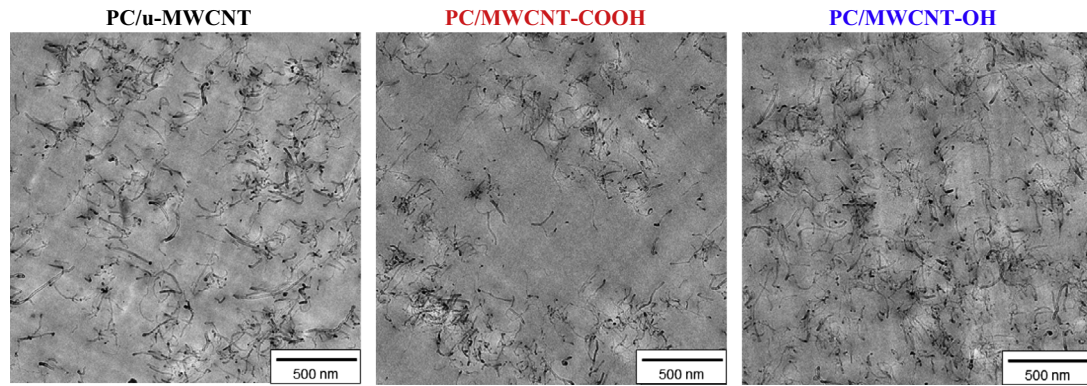


Fig. 3. TEM images of the PC/MWCNT composites showing different states of the MWCNT nano-dispersion due to different functional groups of the MWCNTs.

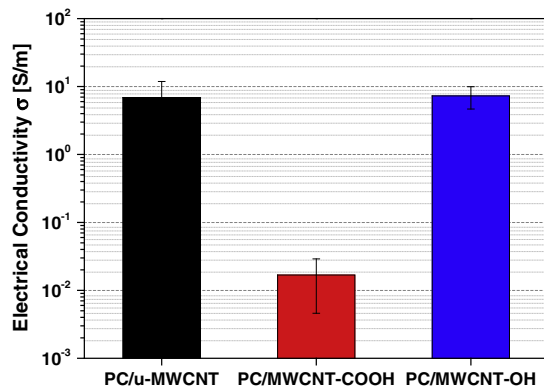


Fig. 4. Electrical conductivity of the composites with 2.5 wt.% MWCNT.

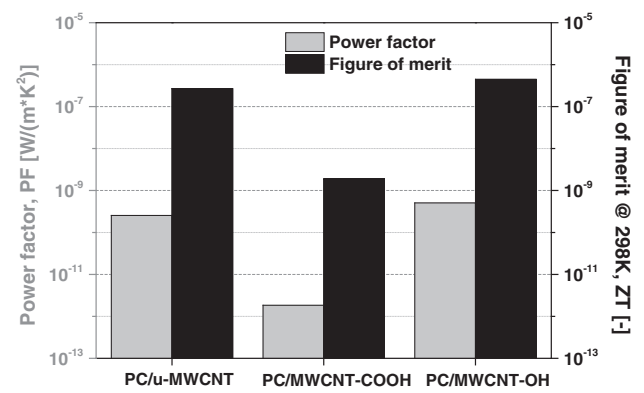


Fig. 6. Power factor (PF) and corresponding figure of merit (ZT) for the different PC/MWCNT composites.

Table 2

Thermal conductivity for PC and the composites with 2.5 wt.% of different MWCNTs.

Sample	Thermal conductivity, $\kappa$ (W/m K <sup>-1</sup> )
PC	0.2 <sup>a</sup>
PC/u-MWCNT	0.28 ± 0.02
PC/MWCNT-COOH	0.29 ± 0.01
PC/MWCNT-OH	0.33 ± 0.01

<sup>a</sup> According to the data sheet of Bayer MaterialScience.

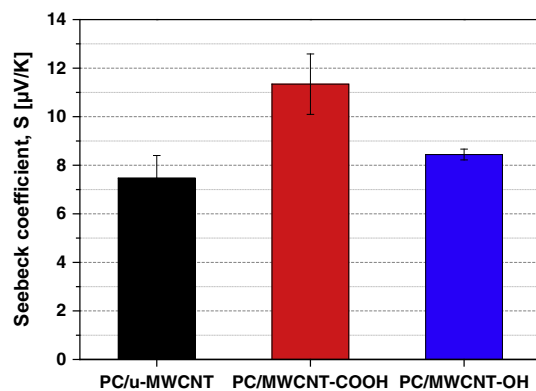


Fig. 5. Seebeck coefficients of composites containing 2.5 wt.% MWCNTs with different functional groups.

are introduced to the MWCNTs as charge carriers and the generated thermovoltage is positive. In other words, the oxygen groups attached on the MWCNTs, both carboxyl as well as hydroxyl, act as p-dopants rendering the MWCNTs p-type semiconductors. The

results are in very good line with observations from the literature, where doping by an acid treatment is shown to improve the Seebeck coefficients of MWCNTs [30,14]. The samples prepared with hydroxyl functionalized MWCNTs show only a slight improvement of the Seebeck coefficient compared to PC/u-MWCNT, due to the relative low amount of oxygen observed with XPS. However, in general it can be deduced that the functional groups stay on the MWCNTs, even after the melt mixing process, to act as a doping and enhance the Seebeck coefficient as compared to non-modified MWCNTs.

In the calculations of power factor (PF) and thermoelectric figure of merit (ZT), the PC/MWCNT-OH sample shows higher values (Fig. 6) than the sample with MWCNT-COOH which can be attributed to the better filler dispersion. However, in general the values of PF and the ZT for the PC/MWCNT-OH are in the same range like those for PC/u-MWCNT, which may be due to similar chemical composition of these commercial fillers. In contrast, the PC/MWCNT-COOH composite shows the lowest PF and ZT, due to the insufficient filler dispersion observed particularly with optical microscopy. However, with an improvement of the filler dispersion, it might be possible to improve the PF and the ZT by several orders of magnitude for this composition.

#### 4. Conclusions

In this study, PC/MWCNT conductive composites with unfunctionalized as well as differently functionalized MWCNTs have been investigated with respect to their use as thermoelectric power generators. The composites were fabricated by a simple and scalable melt-mixing process using commercially available materials.

The thermoelectric efficiency of the composites has been investigated with relation to the MWCNT functional groups, and the composite microstructures. The MWCNT content was kept low at 2.5 wt.% in order to show the correlation between physical properties and morphological observations. In detail, it has been found that the functionalized MWCNTs due to the increased charge carrier density, with the functional groups acting as dopants, resulted in increased Seebeck coefficients up to 52% compared to the unfunctionalized MWCNTs.

The amount of oxygen on the MWCNT surface seems to be crucial for an improvement of the Seebeck coefficient. In addition, the melt mixing, which was applied only for a short time, seems not to affect or decompose the functional groups which were found to endow enhanced thermoelectric properties in the final composites. The thermal conductivity remains, as expected, low in the range <0.5 W/m K and can be considered as a key factor for the utilization of PC/MWCNT composites as thermoelectric materials.

In order to enable the commercialization of the proposed materials, in future, the thermoelectric figure of merit for such composites has to be increased significantly. Therefore, melt-mixed thermoplastics with higher loadings and the use of differently functionalized/doped MWCNTs could be promising to increase the electrical conductivity as well as the Seebeck coefficient. This can be regarded as a possible route to achieve highly efficient polymer/MWCNT thermoelectrics.

## Acknowledgements

We acknowledge the financial support of the DAAD and thank Dr. Maria Omastova (SAS) and Dr. Jürgen Pionteck (IPF) for the possibility to perform the XPS analysis of the used MWCNTs within the “Project Based Personnel Exchange Programme” (PPP) with the topic “Sensors for liquids and vapors based on electric conductive polymer/carbon nanotubes composites”. Furthermore, Dr. Petra Uhlmann and Dr. Wolfgang Jenschke are acknowledged for supplying the temperature gradient stage.

## Appendix A. Supplementary material

Supplementary data associated with this article can be found, in the online version, at <http://dx.doi.org/10.1016/j.compscitech.2014.07.009>.

## References

- [1] Vineis CJ, Shakouri A, Majumdar A, Kanatzidis MG. Nanostructured thermoelectrics: big efficiency gains from small features. *Adv Mater* 2010;22(36):3970–80.
- [2] Boukai AI, Bunimovich Y, Tahir-Kheli J, Yu J-K, Goddard Iii WA, Heath JR. Silicon nanowires as efficient thermoelectric materials. *Nature* 2008;451(7175):168–71.
- [3] Moriarty GP, Wheeler JN, Yu C, Grunlan JC. Increasing the thermoelectric power factor of polymer composites using a semiconducting stabilizer for carbon nanotubes. *Carbon* 2012;50(3):885–95.
- [4] Terry MT. Electrical and thermal transport measurement techniques for evaluation of the figure-of-merit of bulk thermoelectric materials. *Thermoelectrics handbook*. CRC Press; 2005. p. 23–21–23–20.
- [5] Poehler TO, Katz HE. Prospects for polymer-based thermoelectrics: state of the art and theoretical analysis. *Energy Environ Sci* 2012;5(8):8110–5.
- [6] Bubnova O, Khan ZU, Malti A, Braun S, Fahlman M, Berggren M, et al. Optimization of the thermoelectric figure of merit in the conducting polymer poly(3,4-ethylenedioxythiophene). *Nat Mater* 2011;10(6):429–33.
- [7] Dubey N, Leclerc M. Conducting polymers: efficient thermoelectric materials. *J Polym Sci Part B: Polym Phys* 2011;49(7):467–75.
- [8] Hewitt CA, Carroll DL. The effects of acid treatment on the thermoelectric power of multiwalled carbon nanotubes synthesized by chemical vapor deposition. *Chem Phys Lett* 2013;580:67–72.
- [9] Zhao W, Fan S, Xiao N, Liu D, Tay YY, Yu C, et al. Flexible carbon nanotube papers with improved thermoelectric properties. *Energy Environ Sci* 2012;5(1):5364–9.
- [10] Yu F, Hu L, Zhou H, Qiu C, Yang H, Chen M, et al. Thermoelectric power of a single-walled carbon nanotubes rope. *J Nanosci Nanotechnol* 2013;13(2):1335–8.
- [11] Tan X, Liu H, Wen Y, Lv H, Pan L, Shi J, et al. Thermoelectric properties of ultrasmall single-wall carbon nanotubes. *J Phys Chem C* 2011;115(44):21996–2001.
- [12] Mavrinskiy A, Baitinger E. Thermoelectric power in carbon nanotubes. *Semiconductors* 2009;43(4):480–4.
- [13] Kunadian I, Andrews R, Pinar Mengüç M, Qian D. Thermoelectric power generation using doped MWCNTs. *Carbon* 2009;47(3):589–601.
- [14] Nonoguchi Y, Ohashi K, Kanazawa R, Ashiba K, Hata K, Nakagawa T, et al. Systematic conversion of single walled carbon nanotubes into n-type thermoelectric materials by molecular dopants. *Sci Rep* 2013;3.
- [15] Yao Q, Chen LD, Zhang WQ, Liufu SC, Chen XH. Enhanced thermoelectric performance of single-walled carbon nanotubes/polyaniline hybrid nanocomposites. *ACS Nano* 2010;4(4):2445–51.
- [16] Wang L, Jia X, Wang D, Zhu G, Li J. Preparation and thermoelectric properties of polythiophene/multiwalled carbon nanotube composites. *Synth Met* 2013;181:79–85.
- [17] Liang B, Song Z, Wang M, Wang L, Jiang W. Fabrication and thermoelectric properties of graphene/Bi<sub>2</sub>Te<sub>3</sub> composite materials. *J Nanomater* 2013;2013: 5 pages, Article ID 210767.
- [18] Yu C, Kim YS, Kim D, Grunlan JC. Thermoelectric behavior of segregated-network polymer nanocomposites. *Nano Lett* 2008;8(12):4428–32.
- [19] Bounioux C, Díaz-Chao P, Campoy-Quiles M, Martín-González MS, Goñi AR, Yerushalmi-Rozen R, et al. Thermoelectric composites of poly (3-hexylthiophene) and carbon nanotubes with a large power factor. *Energy Environ Sci* 2013;6(3):918–25.
- [20] Choi K, Yu C. Highly doped carbon nanotubes with gold nanoparticles and their influence on electrical conductivity and thermopower of nanocomposites. *PLoS ONE* 2012;7(9):e44977.
- [21] Du Y, Shen SZ, Yang W, Donelson R, Cai K, Casey PS. Simultaneous increase in conductivity and Seebeck coefficient in a polyaniline/graphene nanosheets thermoelectric nanocomposite. *Synth Met* 2012;161(23):2688–92.
- [22] Hewitt CA, Kaiser AB, Roth S, Craps M, Czerw R, Carroll DL. Multilayered carbon nanotube/polymer composite based thermoelectric fabrics. *Nano Lett* 2012;12(3):1307–10.
- [23] Meng C, Liu C, Fan S. A promising approach to enhanced thermoelectric properties using carbon nanotube networks. *Adv Mater* 2010;22(4):535–9.
- [24] Moriarty GP, De S, King PJ, Khan U, Via M, King JA, et al. Thermoelectric behavior of organic thin film nanocomposites. *J Polym Sci, Part B: Polym Phys* 2013;51(2):119–23.
- [25] Abad B, Alda I, Díaz-Chao P, Kawakami H, Almarza A, Amantia D, et al. Improved power factor of polyaniline nanocomposites with exfoliated graphene nanoplatelets (GNPs). *J Mater Chem A* 2013;1(35):10450–7.
- [26] Antar Z, Feller J-F, Noel H, Glouannec P, Elleuch K. Thermoelectric behaviour of melt processed carbon nanotube/graphite/poly (lactic acid) conductive biopolymer nanocomposites (CPC). *Mater Lett* 2012;67(1):210–4.
- [27] Wang L, Wang D, Zhu G, Li J, Pan F. Thermoelectric properties of conducting polyaniline/graphite composites. *Mater Lett* 2011;65(7):1086–8.
- [28] Piao M, Kim G, Kennedy GP, Roth S, Dettlaff-Weglikowska U. Thermoelectric properties of single walled carbon nanotube networks in polycarbonate matrix. *Phys Status Solidi (b)* 2013;250(8):1468–73.
- [29] Piao M, Na J, Choi J, Kim J, Kennedy GP, Kim G, et al. Increasing the thermoelectric power generated by composite films using chemically functionalized single-walled carbon nanotubes. *Carbon* 2013;62:430–7.
- [30] Hewitt CA, Carroll DL. The effects of acid treatment on the thermoelectric power of multiwalled carbon nanotubes synthesized by chemical vapor deposition. *Chem Phys Lett* 2013;580:67–72.
- [31] Piao M, Kim G, Kennedy GP, Roth S, Dettlaff-Weglikowska U. Preparation and characterization of expanded graphite polymer composite films for thermoelectric applications. *Phys Status Solidi (b)* 2013;250(12):2529–34.
- [32] Liebscher M, Tzounis L, Gärtner T, Jenschke W, Müller MT, Stamm M et al. Thermoelectric energy harvesting with highly conductive CNT-filled polycarbonate composites prepared by melt-mixing. In: 6th International conference on carbon nanoparticle based composites, Dresden, Germany, 2013. ISBN 978-3-9816007-0-4.
- [33] Ferreira T, Paiva M, Pontes A. Dispersion of carbon nanotubes in polyamide 6 for microinjection moulding. *J Polym Res* 2013;20(11):1–9.
- [34] Novais RM, Simon F, Paiva MC, Covas JA. The influence of carbon nanotube functionalization route on the efficiency of dispersion in polypropylene by twin-screw extrusion. *Compos A Appl Sci Manuf* 2012;43(12):2189–98.
- [35] Rausch J, Zhuang R-C, Mäder E. Surfactant assisted dispersion of functionalized multi-walled carbon nanotubes in aqueous media. *Compos A Appl Sci Manuf* 2010;41(9):1038–46.
- [36] Ke K, Pötschke P, Jehnichen D, Fischer D, Voit B. Achieving  $\beta$ -phase poly(vinylidene fluoride) from melt cooling: effect of surface functionalized carbon nanotubes. *Polymer* 2014;55(2):611–9.